

# On the dynamics of convolutional recurrent neural networks near their critical point

Aditi Chandra<sup>1,2</sup> and Marcelo O. Magnasco<sup>1</sup>  
<sup>1</sup>*Rockefeller University, New York.* and  
<sup>2</sup>*Physics Department, University of Oxford, UK*

We examine the dynamical properties of a single-layer convolutional recurrent network with a smooth sigmoidal activation function, for small values of the inputs and when the convolution kernel is unitary, so all eigenvalues lie exactly at the unit circle. Such networks have a variety of hallmark properties: the outputs depend on the inputs via compressive nonlinearities such as cubic roots, and both the *timescales of relaxation* and the *length-scales of signal propagation* depend sensitively on the inputs as power laws, both diverging as the input  $\rightarrow 0$ . The basic dynamical mechanism is that inputs to the network generate ongoing activity, which in turn controls how additional inputs or signals propagate spatially or attenuate in time. We present analytical solutions for the steady states when the network is forced with a single oscillation and when a background value creates a steady state of “ongoing activity”, and derive the relationships shaping the value of the temporal decay and spatial propagation length as a function of this background value.

## I. BACKGROUND

Recurrent neural networks (RNNs) are famously difficult [1–3]. While they are Turing universal [4–6], their full potency has been hard to harness due to their complexity. RNNs are difficult to analyze, or predict more than a few steps into the future, and they are difficult to train due to the vanishing gradient problem [1, 2] and related issues. So at present we **neither** have a clear programming paradigm to **design** them, nor a generally effective method to **train** them.

Meanwhile neurobiology confronts us with networks that are almost always recurrent, often heavily so. The need to understand recurrent biological networks has spawned considerable efforts to advance their study. Here we undertake an in-depth description of a very small and simple subset of all RNNs, in the hope it may serve as a beachhead into more general cases.

A concept often discussed in computational neuroscience is *criticality*. One category is *dynamical criticality*, where the real parts of stability parameters approach zero. Two early models are the line attractors [7], where one direction acquires a zero eigenvalue, and the Hopf bifurcation scenario for hair-cell dynamics [8–10], where the eigenvalues are purely imaginary. Since then, there’s been continued interest in this scenario, both theoretically [11–14] as well as experimentally [15–18], and it’s been conjectured to be involved in dynamical reconfiguration and functional flexibility [19, 20]. Furthermore, it has been argued that traveling waves play an essential role in the theory of recurrent neural networks. both in terms of maintaining the “working memory” of the RNN [21] as well as transferring information between working variables [22]. Traveling waves are sustained by dynamically critical eigenmodes.

While many models of neuronal function are written as continuous-time differential equations, artificial neural networks are usually expressed by discrete-time recurrences. Moving from continuous- to discrete-time requires an exponentiation operation: purely imaginary (critical) eigenvalues are mapped by the exponential to

lay on the unit circle [23], and connectivities are mapped to orthogonal or unitary matrices; see [14, 24] for an explicit derivation applicable to our case. There has been a lot of recent interest from the ML community in recurrent networks with either orthogonal or unitary evolutions [25–28]; as maintaining orthogonality is algorithmically difficult (a.k.a. the parametrization of the Stiefel manifold), even initializing the weights to be orthogonal or unitary helps with subsequent evolution of the training [29–31]. Here we will explore a model for which establishing and maintaining unitarity is algorithmically fast [24].

## II. THE MODEL

A complex-valued layer  $Z$  whose structure supports convolutions (e.g. square lattices in  $D$  dimensions with periodic boundary conditions) evolves through the discrete-time recurrent dynamics

$$Z_{n+1} = \phi(U \otimes Z_n + I_n) \quad (1)$$

where  $Z_n$  denotes the values of the layer at time  $n$ ,  $U$  is a convolution kernel,  $\otimes$  is the convolution operation native to  $Z$ , and the activation function  $\phi$  is an *element-wise* function given by

$$\phi(z) = \frac{z}{\sqrt{1 + |z|^2}} \quad (2)$$

We will want a convolution kernel  $U$  whose action, when viewed as a linear operator, is *unitary*. A computationally fast way to generate unitary convolutions [24] is to use the *convolutional exponential*  $e_{\otimes}^A$  applied to an anti-Hermitian kernel  $A$ ; this can be explicitly computed in Fourier space as

$$U = e_{\otimes}^A \equiv \mathcal{F}^{-1} [\exp(\mathcal{F}[A])] \quad \text{with} \quad A^\dagger = -A \quad (3)$$

with the exponentiation in the rhs taken element-wise. The anti-Hermitian kernel  $A$  reverses sign upon flipping

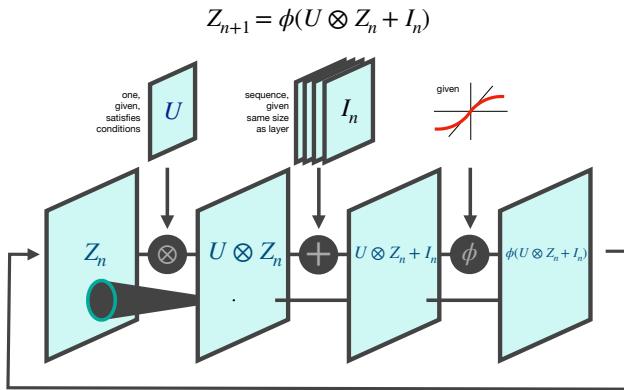


Figure 1. Schematic of the map Eq 1. For any given element in the layer, all the inputs are added together; the inputs from other elements in the layer is given by the convolution, and the external input is added element-wise. Finally the activation function is applied, and the result becomes the values of the layer for the next time-step.

centrally and complex-conjugating. See Figure 1 The convolutional exponential is a fast  $N \log N$  operation. All eigenvalues of a unitary operator have absolute value equal to 1 and therefore the operator does not expand or contract any direction; in dynamical systems parlance, it satisfies Liouville’s theorem and preserves phase space volume, with expansions or contractions only coming locally from the slope of  $\phi$ . In fact with these choices of activation and kernel, Eq. 1 is time-reversible.

In the theory of ML, equation 1 is a convolutional recurrent neural net, where the emphasis is on training the weights  $U$  (or better stated,  $A$  if we want to keep the system unitary) while in the theory of dynamical systems it is a *coupled map lattice* [32, 33], where the emphasis is on complex asymptotic behavior upon use of chaotic maps  $\phi$ .

### A. Notation

In the rest of this paper we shall (ab)use the following notation introduced in [24], which is regrettably necessary as it is very easy to get confused. A one megapixel image, despite being arranged in 2D, is **not actually a matrix** because we do not rely on multiplying two images together using matrix multiplication – using the dot products of the first one’s rows with the second one’s columns. It is a 2D *array*, but *not* an actual *matrix* embodying a linear algebra operator over a vector space. For our analysis it is a *vector* with 1 million elements, an element of the vector space of all possible images. Similarly, a 2D convolution kernel looks like a matrix but it actually isn’t. It is an element of the vector space of kernels, and possesses a central element, which we will call  $(0, 0)$ , which is the kernel element that gets multiplied by *this* pixel when convolving. We’ll use Python notation in referring to elements to the left and below

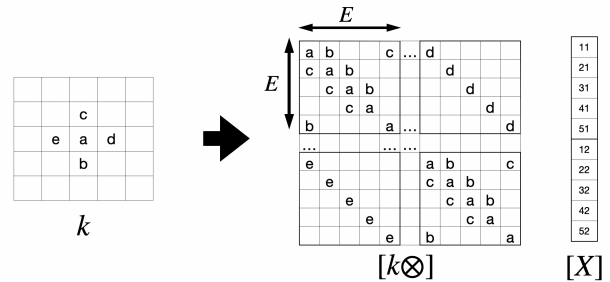


Figure 2. Choose as a basis the “reshape” operation from an  $E \times E$  square to a vector of length  $E^2$  ( $0 \leq i < E, 0 \leq j < E$ )  $\rightarrow k \equiv i + E j < E^2$  and a convolution which for every point in the lattice adds up the first neighbors with coefficients  $y_{ij} = ax_{ij} + bx_{i+1,j} + cx_{i-1,j} + dx_{ij+1} + ex_{ij-1} \quad \forall ij$ . This operation maps the kernel onto a sparse array with lots of repetitive diagonal structures and off-diagonal stuff for boundary conditions. Any matrix property invariant under change of basis is a property of the kernel too. For example, transposition  $\rightarrow$  central symmetry.

this center as having negative indices. OTOH the operation of convolving with a kernel  $K$ , denoted abstractly as  $K \otimes$ , is indeed a proper operator in the sense of linear algebra, and hence it is (abstractly) a matrix if we were to express it in any given basis; it is a matrix of 1 million rows times 1 million columns with a characteristically repetitive structure and lots of empty space, so we never actually write it out that way because it is wasteful, but that is what it is.

We shall denote by  $Z$  and  $U$  the layer and the kernel in their “natural” topology, e.g. as 1D or 2D arrays. However, it will be useful throughout to choose a basis for the vector space of all  $Z$ s, and we shall denote by  $[Z]_B$  the representation of  $Z$  in the basis  $B$ ; this representation is always a vector regardless of the dimensionality of  $Z$ . The dimension of this representation is the total number of elements in the layer: the vector representing a 1D layer of size  $N$  has  $N$  elements and looks the same as the original, and a 2D layer of width  $W$  and height  $H$  has  $W \times H$  elements. There is one canonical basis for  $Z$  in 1D: the layer itself laid out as a vector. In 2D, there are two canonical bases: the “Fortran” or “column-major” basis, which takes each column of  $Z$  as a vector and concatenates them sequentially, or the “C” or “row-major” basis, where it is now the rows who are concatenated one after the other. We declare ourselves agnostic on this quasi-religious issue. The other basis that we shall need to use is the Fourier basis, which we shall call  $\mathcal{F}$ , and which will denote Fourier transformation in the dimension appropriate to the layer and in the same major order that is used for the layer.

The operation of convolving an object with some kernel  $K$ , which we could call  $K \otimes$  (“ $K$  convolved with”) is a linear operator;  $[K \otimes]_B$  is the representation of this linear operator on the basis  $B$ , and it is a *square matrix* whose sides are equal to the total number of elements

of  $Z$ . See Figure 2. In the 1D case, it is an  $N \times N$  matrix, in the 2D case a  $WD \times WD$  matrix. Using this notation,

$$[K \otimes Z] = [K \otimes] \times [Z]$$

where  $\times$  is matrix multiplication:  $[K \otimes Z]$  is a vector obtained by matrix multiplication of the matrix  $[K \otimes]$  times the vector  $[Z]$ . It is computationally inefficient to do it this way, but this what the convolution is. Any matrix property of  $[K \otimes]$  which is invariant under change of basis, e.g. its eigenvalues, can therefore be properly attributed to  $K$  itself, and so henceforth we will refer to “the eigenvalues of  $K$ ” meaning  $\text{eig}([K \otimes])$ ; under no circumstance should it be interpreted as the eigenvalues of the array where  $K$  is stored. In addition, the operation of flipping  $K$  “antipodally” through its center (element “(0,0)”, the element that multiplies the same pixel we are assigning to in the convolution), call it  $K^F$  corresponds, in any dimension, to transposing  $[K \otimes]$ , thus allowing us to use the words “symmetric” or “Hermitian” as applied to  $K$ : it is not a transpose of the array storing  $K$  but rather a central flip swapping each element with its antipode. Thus  $[K^F \otimes] = [K \otimes]^T$ .

Since matrix multiplication of the representation is the representation of the application of the convolution it follows that

$$[(K \otimes K) \otimes] = [K \otimes] \times [K \otimes]$$

and so on for all powers, from where, by summing order by order the Taylor series of the matrix exponential,

$$e^{[K \otimes]} = I + [K \otimes] + \frac{[K \otimes]^2}{2!} + \frac{[K \otimes]^3}{3!} + \dots$$

we define  $e_{\otimes}^K$ , the *convolutional exponential* of  $K$  as the kernel whose representation equals the matrix exponential of the representation of  $K \otimes$ :

$$[e_{\otimes}^K] \equiv e^{[K \otimes]}$$

from where

$$e_{\otimes}^K \equiv 1 + K + \frac{K \otimes K}{2!} + \frac{K \otimes K \otimes K}{3!} + \dots$$

Recurrent use of the Fourier convolution theorem,  $K \otimes K = \mathcal{F}^{-1}[\mathcal{F}[K]^2]$ , gives us  $K \otimes K \otimes K = \mathcal{F}^{-1}[\mathcal{F}[K]^3]$  and so on and so forth, and summing all orders gives Eq. 3.

Therefore, in order to generate a unitary kernel, we take an arbitrary *real* kernel  $K$  and

$$K \rightarrow A = \frac{K - K^F}{2} + i \frac{K + K^F}{2} \rightarrow U = e_{\otimes}^A \quad (4)$$

with the first step being fully invertible.

### III. BASIC ANALYSIS

A number of basic considerations were elaborated in [24] which we will not repeat here; we add here what we need for this Paper.

#### A. Choice of activation function $\phi$

This model is based on a discrete-time dynamics; and correspondingly we have chosen the activation function  $\phi$  to correspond to the discrete-time dynamics of a marginally-stable fixed point. To derive  $\phi$ , consider the equation  $\dot{z} = -|z|^2 z$ . Being rotationally invariant we can assume  $z$  to be real and positive. Being 1D it admits a closed-form solution in quadratures:

$$\begin{aligned} \frac{dz}{-z^3} = dt &\rightarrow \int_{z(0)}^{z(t)} \frac{dz}{-z^3} = \int_0^t dt \rightarrow \\ &\rightarrow (z(t)^{-2} - z(0)^{-2}) = 3t \end{aligned}$$

from where we obtain the solution and cast it as a flow  $\phi_t$ :

$$z(t) = \frac{z(0)}{\sqrt{1 + 3tz(0)^2}} \rightarrow \phi_t(z) \doteq \frac{z}{\sqrt{1 + 3t|z|^2}}$$

Being a flow, i.e. the outcome of integrating an ODE, it comes equipped with a *group structure*: evolving to  $t_1 + t_2$  is the same as evolving to  $t_1$  and then evolving  $t_2$  more:

$$\phi_{t_1} \circ \phi_{t_2} = \phi_{t_1+t_2} \quad (5)$$

and is invertible:

$$\phi_t^{-1} = \phi_{-t} = \frac{z}{\sqrt{1 - 3t|z|^2}}$$

Finally,  $\phi$  and rotations commute:

$$\phi(e^{i\theta} z) = e^{i\theta} \phi(z) \quad (6)$$

so  $\phi$  gives us the exact analytical solution to the (unforced) Hopf normal form.

In the remainder of this paper we choose  $t = 1/3$  and we drop the time index.

#### B. Compression and singularity

A compressive power law amplifies small values and attenuates large values, because the derivative of  $x^\alpha$  for  $\alpha < 1$  diverges as  $x \rightarrow 0$  and conversely approaches 0 as  $x \rightarrow \infty$ , hence the name *compression*. One classic example is Galileo’s observation of relief in the Moon, as the glancing incidence of light at the terminator line amplifies relief; if the relief is about  $h$  in height and the terminator line wanders  $W$  from the median, then  $W = \sqrt{2hR}$ , so if the relief is  $5km$  in height, then  $W = \sqrt{2 \times 5km \times 1740km} \approx 132km$ .

Critical systems display powerful compressive nonlinearities; for example, a system poised exactly at a Hopf bifurcation, while forced exactly at the resonant frequency, displays a cubic root response [9]. Naturally

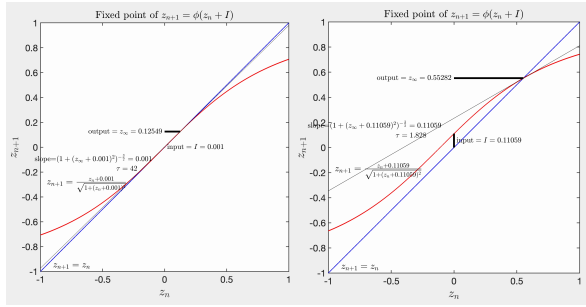


Figure 3. Fixed point and slope at the fixed point. In these diagrams, the fixed point lies at the intersection of the curve with the diagonal; as the input displaces the curve upwards, the fixed point moves to the right. Left, with a very small input (0.001) representing a nearly invisible displacement of the curve with respect to the diagonal, the fixed point moves right by  $(2 * 0.001)^{1/3} = 0.12549$ , and the slope at the fixed point gives a relaxation time of 42 iterations. Right, a much larger input of 0.11 gives rise to a displacement of 0.55, with a relaxation time of 1.8 iterations.

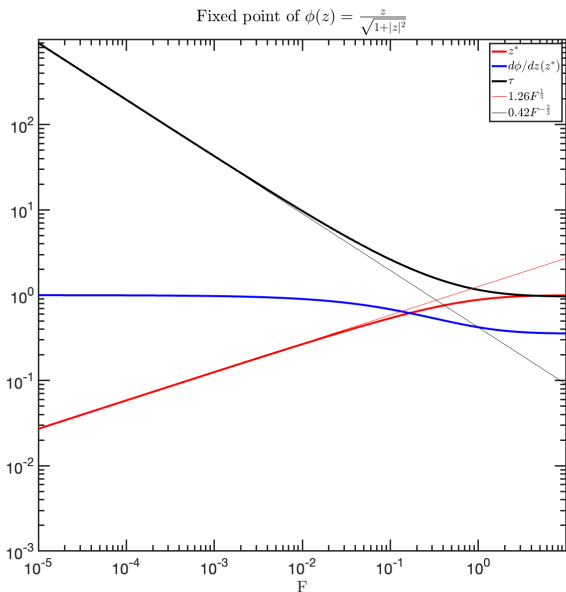


Figure 4. Fixed point and slope at the fixed point, as a function of input.

this behavior extends to our system. Consider the 1D recurrence

$$z_{n+1} = \phi(z_n + I) = \frac{z_n + I}{\sqrt{1 + (z_n + I)^2}} \quad (7)$$

Because all slopes are  $\leq 1$  this recurrence is a contraction, and has a single fixed point  $z^* = \phi(z^* + I)$ , which leads to

$$I = \phi^{-1}(z^*) - z^*$$

where  $\phi^{-1}(z) = z/\sqrt{1 - z^2}$ .

Because the slope of  $\phi$  at the origin is 1, and therefore is tangent to the diagonal line, adding a tiny  $I$  will displace the fixed point by a considerable amount, as illustrated in Figure 3; in fact proportional to  $(2I)^{1/3}$  for small enough  $I$ , as can be seen by expanding

$$I = \frac{z^*}{\sqrt{1 - z^{*2}}} - z^* \approx \frac{z^{*3}}{2} + \frac{3z^{*5}}{8} + \frac{5z^{*7}}{16} + O(z^{*9})$$

where for sufficiently small  $I$  then

$$z^* \approx (2I)^{1/3} \quad (8)$$

The slope at the fixed point then is  $\phi'(z^* + I) = (1 + (z^* + I)^2)^{-3/2}$ ; the decay time  $\tau$  is defined by  $\phi'^\tau = e^{-1}$  or  $\tau = -1/\log(\phi')$ , and with  $\log\left((1 + (z^* + I)^2)^{-3/2}\right) \approx -\frac{3}{2}(z^* + I)^2 \approx -\frac{3}{2}(2I)^{2/3}$  then we get

$$\tau \approx \frac{2}{3}(2I)^{-2/3} \quad (9)$$

This equation then defines that *the timescale of relaxation in this system is a function of the input*. See Figure 4.

### C. The eigenvalues of $U \otimes$

As described above in Notation, the representation of  $[K \otimes]$  is a matrix and thus it has eigenvalues and eigenvectors. We now will show exactly what these are.

The Fourier Convolution theorem states that the Fourier transform of a convolution is the point-wise product of the Fourier transforms. In our specific case, it means that we can FFT the layer  $Z$  and the kernel  $K$  and element-wise multiply them. Abusing our notation yet again,

$$[K \otimes Z]_{\mathcal{F}} = [K]_{\mathcal{F}} .* [Z]_{\mathcal{F}}$$

where the  $.*$  operator is point-wise multiplication of two vectors and the subscript means “in the Fourier basis”. How can we reconcile this with

$$[K \otimes Z]_{\mathcal{F}} = [K \otimes]_{\mathcal{F}} \times [Z]_{\mathcal{F}}$$

where  $[K \otimes]_{\mathcal{F}}$  is a matrix and  $\times$  is matrix multiplication? The way to promote point-wise multiplication by a vector to matrix multiplication is if the matrix is diagonal:

$$[K \otimes]_{\mathcal{F}} = \text{diag}([K]_{\mathcal{F}})$$

where the  $\text{diag}$  operation is to embed a vector as the main diagonal of a matrix leaving all other elements zero.

Therefore *the elements of the Fourier transform of the kernel  $K$  are the eigenvalues of the matrix  $[K \otimes]$  and thus of the kernel  $K$  itself*. And, since the representation

$[K \otimes]_{\mathcal{F}}$  is diagonal in the Fourier basis, the eigenvectors of  $K$  are *the Fourier basis functions themselves*, namely  $e^{2\pi i \frac{k_j}{n}}$  etc. This is a direct result of the translational invariance of the convolution operation.

All of the computational advantages of the present model are given by the ability to diagonalize (an  $N^3$  operation in general) by Fast Fourier transformation (an  $N \ln N$  operation). Evidently, since any kernel  $K$  is diagonal on the same Fourier basis, all convolutions commute as they share eigensystems.

#### D. Perturbation analysis using a unitary $U$

A small perturbation to the initial condition  $Z_0$  propagates forward using the chain rule[23]

$$\frac{\partial Z_n}{\partial Z_0} = \prod_{i=0}^{n-1} \Lambda_i [U \otimes]$$

where the  $\Lambda_i$  are diagonal matrices whose elements are

$$\Lambda_i = \text{diag} \left( \left. \frac{\partial \phi}{\partial x} \right|_{x_i} \right) = \text{diag}(\phi'(U \otimes Z_i + I_i))$$

For small values of the activities, the elements of  $\Lambda$  are close to 1, and so the evolution is determined by the eigenvalues of  $[K \otimes]$  and whether their powers diverge or go to zero is determined exclusively by their absolute values. It is therefore of interest to use kernels all of whose eigenvalues have unit absolute value. Generating unitary matrices, otherwise known as the Stieffel manifold parametrization problem, is computationally expensive in the general case, as the simplest method is through exponentiation of an anti-Hermitian matrix. On the other hand as shown above, unitary kernels can be generated by using the convolutional exponential, which is fast because kernels are diagonal in the Fourier basis and so FFT can be used.

#### E. Dispersion relation

The FFT of the kernel gives the resonance frequencies, so plotting these as a function of  $(k_x, k_y)$  literally draws out the dispersion relation.

We will examine some number of kernels, including the standard  $i\Delta$ , the diffractive coupling or free Schrödinger equation, plus various couplings with random elements. One specific random kernel we shall come back to using consists of random numbers within a disk of radius  $R$  and zero outside. This allows the kernel to be somewhat local, and the frequencies to vary continuously in  $(k_x, k_y)$  space.

Finally note the most important distinction is whether the antiHermitian generator for the kernel  $K$  is purely imaginary (symmetric) or purely real (antisymmetric) or full antiHermitian (a linear combination of both).

## IV. RESULTS

### A. Resonance and nonlinear compression

Consider forcing the system 1 with a periodic force of amplitude  $\alpha$  and frequency  $e^{i\theta}$  at one single site, e.g. the origin:

$$I_n = \alpha e^{in\theta} \delta_0 \quad (10)$$

where  $\delta_0$  is an array the same size as the layer with a single 1 at site 0 and zero otherwise. When  $\alpha \ll 1$  and the frequency  $e^{i\theta}$  coincides exactly with an eigenvalue of  $K$ , then the system resonates and the growth is only limited by reaching the nonlinear regime of  $\phi$ . These resonances show the characteristic 1/3-power law scaling and width broadening described in detail in [9]. See Figure 5

We will revisit this subject later in order to derive an analytical solution to this diagram.

### B. Background-dependent wave attenuation

We now consider an input consisting of a fixed constant background  $I^*$  plus a small input  $I_n = I^* + S_n$  where  $S_n \ll 1$ . We follow standard dynamical systems perturbation theory

$$Z_{n+1} = \phi(U \otimes Z_n + I_n)$$

we compute the fixed point for the input  $I^*$  alone

$$Z^* = \phi(U \otimes Z^* + I^*)$$

and since a constant input is always an eigenvector of  $[U \otimes]$ , calling its eigenvalue  $\lambda_0$ , we get  $Z^* = \phi(\lambda_0 Z^* + I^*)$  which is now a scalar equation. We will then denote the response to  $I_n = I^* + S_n$  as  $Z_n = Z^* + R_n$ , and substituting

$$Z^* + R_{n+1} = \phi(U \otimes Z^* + U \otimes R_n + I^* + S_n)$$

and assuming that  $R_n$  is also small (not true at resonance) we can expand to 1st order to get

$$Z^* + R_{n+1} = \phi(\lambda_0 Z^* + I^*) + \phi'(\lambda_0 Z^* + I^*)(U \otimes R_n + S_n)$$

where the constant slope of the activation function at the fixed point

$$\gamma \doteq \phi'(\lambda_0 Z^* + I^*) \quad (11)$$

will be called  $\gamma$ , from where we get the linear equation

$$R_{n+1} = \gamma(U \otimes R_n + S_n)$$

Since this equation is diagonal in Fourier space, using tildes to denote the (spatial) Fourier transforms (e.g.  $\tilde{R} = \mathcal{F}[R]$ ) we get

$$\tilde{R}_{n+1} = \gamma \tilde{U} \tilde{R}_n + \gamma \tilde{S}_n \quad (12)$$

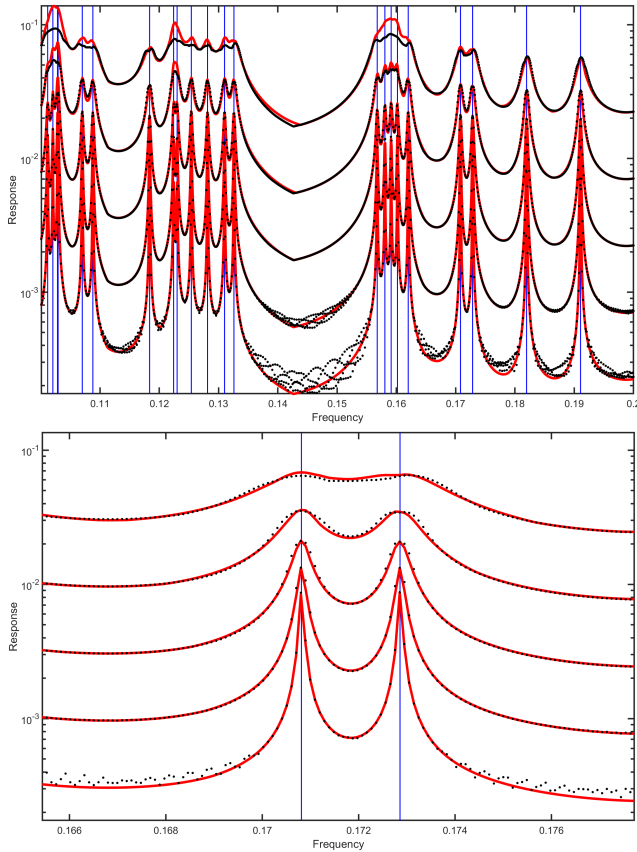


Figure 5. The eigenvalues of  $K$  are resonance frequencies of the system, in that forcing at exactly that frequency causes the system to give a disproportionately large response. Resonances of the system show compressive nonlinearities at the resonances, linear behavior away from the resonances, and broadening of the responses as the forcing amplitude increases to match both regimes to each other. Shown are the amplitude of the responses to 5 different intensities separated by  $\sqrt{10}$  from each other. Black dots are the result of numerical simulation ( $N=1024$ , completely random  $K$ ,  $2^{24}$  iterations, 1024 frequencies, 5 intensities  $10^{-(1:5)/2}$ ). Red lines are the analytical calculation of Eq. 14. The blue lines are the eigenvalues of the kernel. Bottom panel: detail showing the widening as the amplitude of the input increases.

where the product between the Fourier transforms of the kernel and the perturbation is again *element-wise*. Remembering that the Fourier transform of the kernel consists of its eigenvalues as a linear operator and that, in the case we have hitherto considered in which  $U = e^{\otimes A}$  is the convolutional exponential of an anti-Hermitian kernel. Evidently  $|\gamma| < 1$  is needed for a stable solution to this perturbative equation.

There is a slight issue though:  $\phi$  is not an analytic function, and thus its derivative is not the same in every direction. The derivative of  $\phi$  is  $\gamma$  along the radial direction, but along the angular direction Eq. 6 prescribes the derivative to be  $i/\sqrt{1+x^2}$ . As the argument continuously rotates, an effective  $\gamma$  ensues, which is  $\gamma_{\text{eff}} = (1 + 2\gamma)/3$ .

### C. Attenuation of periodic single-site forcing

Consider the sub-case in which  $S_n$  is applied at a single site (wlog the origin) and is a periodic function of time;  $S_n = \alpha e^{in\theta} \delta_{j_0}$  where  $j$  is an index into the layer's individual elements, and we expect that asymptotically the response will also oscillate like  $R_n \approx R^* e^{in\theta}$ . The spatial Fourier transform of  $\delta_{i_0}$  is a constant vector. Substituting

$$\tilde{R}^* e^{in\theta} e^{i\theta} = \gamma_{\text{eff}} \tilde{U} \tilde{R}^* e^{in\theta} + \gamma_{\text{eff}} \alpha e^{in\theta} \tilde{\delta}$$

where again multiplication is element-wise element-wise leads to the solution

$$\tilde{R}^* = \cdot \frac{\gamma \alpha \mathbf{1}}{(e^{i\theta} - \gamma_{\text{eff}} \tilde{U})}$$

where the period in front of the division sign reminds us again that this division is *element-wise*. Inverting the FFT

$$R^* = \mathcal{F}^{-1} \left[ \frac{\alpha \mathbf{1}}{e^{i\theta} / \gamma_{\text{eff}} - \tilde{U}} \right] \quad (13)$$

The closer  $e^{i\theta}$  is to an eigenvalue of  $K$  and the closer  $\gamma$  is to 1 we approach a resonant situation. For kernels with a smooth dispersion relation, like a Laplacian kernel,  $R^*$  decays exponentially away from the site of injection like  $e^{-\lambda|x|}$ ; the spatial decay constant  $\lambda$  is inversely proportional to the temporal decay constant  $\tau \equiv -1/\log \gamma$  through the group velocity  $\partial\omega/\partial k$ , or otherwise the density of eigenvalues around the forcing frequency. Please see Figure 6, where both full numerical simulations as well as this analytical solution for various intensities of  $I^*$  and thus of  $\gamma$ . Fitting straight lines to the flanks of  $R^*$  to obtain  $\lambda$  we observe that indeed  $\lambda \approx 1/\tau$ . In Figure 7, the value of  $c_{\text{eff}} \doteq 1/(\lambda\tau)$  is computed for various different forcing frequencies, and shown to agree exactly with the value of the group velocity  $c_g \doteq \partial\omega/\partial k$ , which for this particular kernel equals  $\frac{3}{2}\sqrt{\omega(\pi-\omega)}$ .

### D. Periodic forcing at one single element, analytic solution

Equipped with Equation 13, we can now attack again the problem of the responses to a single frequency at a single point, but with no background activity. As described above, the response will grow in time until it saturates, and it will saturate at a level that is nonlinearly dependent on the amplitude of the incoming oscillation through a compressive nonlinearity of order  $1/3$ . In steady state,

$$R^* e^{in\theta} e^{i\theta} = \phi(U \otimes R^* e^{in\theta} + \alpha e^{in\theta} \delta_{i_0})$$

We will now investigate whether these steady state solutions conform to 13; by inverting Equation 13, we

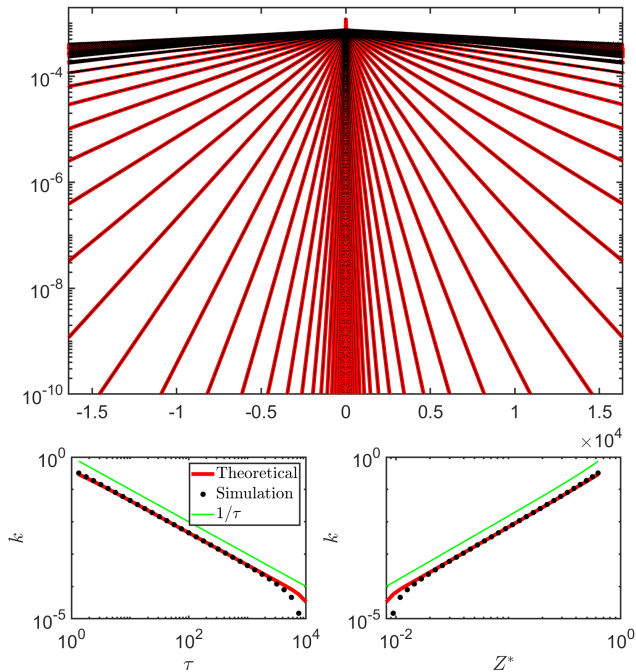


Figure 6. Attenuation of a propagating wave. Top panel, an oscillatory forcing is injected at the center, and propagates outwards, attenuating as it does. In the asymptotic state, away from the injection site  $R^* \approx e^{-\lambda|x|}$ . The different lines were generated by choosing  $\tau = 10^{(1.32)/8}$  and generating the corresponding  $I^*$ .  $N = 2^{16}$ ,  $\alpha = 10^{-3}$ ,  $U = e^{i\Delta}$ ,  $\lambda = e^{-i}$ . Black dots, full numerical simulation,  $2^{17}$  timesteps. Red solid curves, from Eq. 13. Bottom left,  $\lambda$  vs.  $\tau$  show an inverse relationship. Green line is  $1/\tau$ . Bottom right, direct power law between  $\lambda$  and  $Z^*$ .

get a simple diagnostic for whether this solution obeys this expression:

$$\left( \frac{\alpha}{\mathcal{F}[R^*]} + \tilde{U} \right) e^{-i\theta} = \gamma^{-1}$$

or, namely, every single element of the expression on the left should be equal to  $1 + \epsilon$  with  $\epsilon \ll 1$ . Numerical simulation shows this is indeed the case, although it takes an extremely long time to converge for most elements when the  $\alpha$  is very small. However, the element closest to the driving frequency (the pole) converges rather rapidly because it is largest in amplitude; furthermore it shows that  $\epsilon$ , which measures the distance to the unit circle, is a power law:  $\epsilon = PN^{-2/3}\alpha^{2/3}$ , with the proportionality constant  $P$  being of order 1 and dependent only on the degeneracy of the eigenvalue (i.e. in 1D  $P = (1/2)^{1/3}$  for non-degenerate eigenvalues, or  $P = (3/2)^{1/3}$  for a purely imaginary symmetric  $aH$ , where the eigenvalues are two-fold degenerate)

Therefore we can reconstruct the solution using Equation 13 and using

$$\gamma^{-1} = 1 + P \left( \frac{\alpha}{N} \right)^{\frac{2}{3}}$$

namely

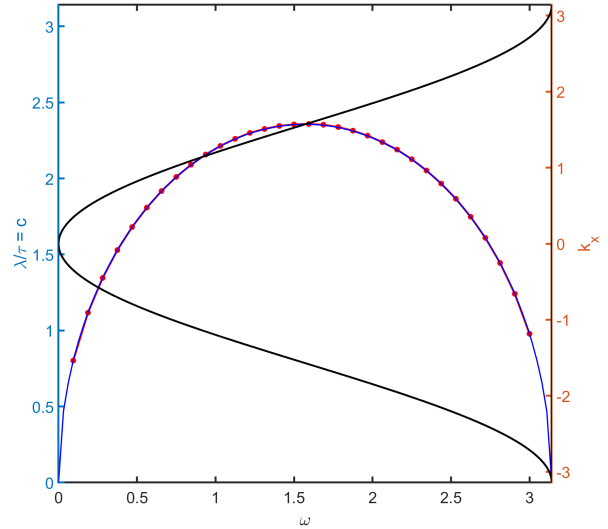


Figure 7. As shown in the prior figure, the decay lengthscale  $\lambda$  is proportional to  $1/\tau$ ; the value of  $1/(\lambda\tau)$  has units of space/time and is a speed  $c_{eff}$ . For multiple values of  $\omega$  and  $\tau$  the propagation solutions were computed, and linear fits to the log of  $|R^*|$  were used to evaluate  $\lambda$ . At any given frequency,  $c_{eff}$  was estimated as the median of  $1/(\lambda\tau)$  for that frequency and all  $\tau$ . Left axis,  $c_{eff}$  vs. the forcing frequency (red), and  $c_g \doteq \partial\omega/\partial k = \frac{3}{2}\sqrt{\omega(\pi-\omega)}$  (blue). Right axis, rotated dispersion relation for the  $U = e^{i\Delta}$ , where it can be seen that  $\omega = \frac{\pi}{2}(\cos(k) - 1)$ .

$$R^* = \mathcal{F}^{-1} \left[ \frac{\alpha \mathbf{1}}{\left(1 + P \left(\frac{\alpha}{N}\right)^{\frac{2}{3}}\right) e^{i\theta} - \tilde{K}} \right] \quad (14)$$

Figure 5 shows the close agreement between this solution and the numerical simulations. The analytic solution deviates slightly from the numerical calculations at the largest values of  $\alpha$  and exactly on the resonances, where the amplitude of the solution no longer follows the power law. Elsewhere the agreement is full.

## V. CONCLUSIONS

If you raise the cover of a piano, depress the right pedal to lift the felt dampers from the strings, and then loudly yell into the back, you'll hear the strings resonate sympathetically with the components of your voice; for several seconds after your vocalization you'll hear a memory of the timbral characteristics of it. If you yell at a different pitch it will keep a different memory. This classical demonstration of resonance and spectral decomposition is, in its own way, a demonstration of memory. As a dynamical mechanism it is diametrically opposite to the Hopfield network; reverberation

stores information in center manifolds as opposed to fixed points.

However the purely resonant memory does not explicitly retain the passage of time; for that we need *propagation* in addition to resonance, so that a position in space encodes time elapsed. The cuRNNs discussed in this Paper provide such propagation; this is more explicit when the kernel is spatially compact, but for kernels with bigger spatial support, information is still *reversibly* scrambled as time elapses, by scrambling phases of oscillations. Recent studies have found a central role to wave propagation in both instantiating a “working memory” of the RNN [21] as well as transferring information between working variables as well as storing it [22]. These traveling waves are naturally associated to eigenvalues of the synaptic matrix of unit absolute value. It is considerably easier to study such traveling waves in a convolutional system, as the fast convolutional exponential allows us both to generate the unit eigenvalues that support such waves, as well as re-

lating those eigenvalues directly to the eigenvector that represents its support in the units.

The center concern of this Paper has been the modulation of spatial and temporal scales by the action of the input. In a critical system, there are no natural timescales or lengthscales, both being formally infinite; external inputs then lower these to finite values through interactions between the input and the nonlinear terms. Input-dependent changes in spatial propagation and relaxation timescales have been experimentally observed e.g. in primary visual cortex [34–37], and some features thereof have been found to agree with critical models [12, 13], yet comprehensive fundamental theories are still at large. We have given here a pretty complete analytic treatment of how timescales and lengthscales of traveling waves are dynamically modulated by ongoing activity, as a direct consequence of the critical nature of our system. In oncoming work we shall show how such ongoing activity can be spatially patterned to dynamically create channels for these waves.

- 
- [1] Pascanu, Razvan; Mikolov, Tomas; Bengio, Yoshua (21 November 2012). "On the difficulty of training Recurrent Neural Networks". arXiv:1211.5063
- [2] Hochreiter, S.; Bengio, Y.; Frasconi, P.; Schmidhuber, J. (2001). "Gradient flow in recurrent nets: the difficulty of learning long-term dependencies". In Kremer, S. C.; Kolen, J. F. (eds.). *A Field Guide to Dynamical Recurrent Neural Networks*. IEEE Press. ISBN 0-7803-5369-2. Medsker, L. R., & Jain, L. C. (2001). *Recurrent neural networks. Design and Applications*, 5(64-67), 2.
- [3] Salehinejad, H., Sankar, S., Barfett, J., Colak, E., & Valaee, S. (2017). Recent advances in recurrent neural networks. arXiv preprint arXiv:1801.01078.
- [4] Siegelmann, Hava T., and Eduardo D. Sontag. "Turing computability with neural nets." *Applied Mathematics Letters* 4.6 (1991): 77-80.
- [5] Kilian, J., & Siegelmann, H. T. (1996). The dynamic universality of sigmoidal neural networks. *Information and computation*, 128(1), 48-56.
- [6] Stogin, J., Mali, A., & Giles, C. L. (2024). A provably stable neural network Turing machine with finite precision and time. *Information Sciences*, 658, 120034.
- [7] Seung, H. S. (1996). How the brain keeps the eyes still. *Proceedings of the National Academy of Sciences*, 93(23), 13339-13344.
- [8] Choe, Yong, Marcelo O. Magnasco, and A. J. Hudspeth. "A model for amplification of hair-bundle motion by cyclical binding of Ca<sup>2+</sup> to mechano-electrical-transduction channels." *Proceedings of the National Academy of Sciences* 95.26 (1998): 15321-15326.
- [9] Eguíluz VM, Ospeck M, Choe Y, Hudspeth AJ, Magnasco MO. Essential nonlinearities in hearing. *Physical review letters*. 2000 May 29;84(22):5232.
- [10] Magnasco, Marcelo O. "A wave traveling over a Hopf instability shapes the cochlear tuning curve." *Physical review letters* 90.5 (2003): 058101.
- [11] Magnasco, Marcelo O., Oreste Piro, and Guillermo A. Cecchi. "Self-tuned critical anti-Hebbian networks." *Physical review letters* 102.25 (2009): 258102.
- [12] Yan, Xiao-Hu, and Marcelo O. Magnasco. "Input-dependent wave attenuation in a critically-balanced model of cortex." *PloS one* 7.7 (2012): e41419.
- [13] Hayton, Keith, Dimitrios Mirogiannis, and Marcelo Magnasco. "Adaptive scales of integration and response latencies in a critically-balanced model of the primary visual cortex." *Plos one* 13.4 (2018): e0196566.
- [14] Alonso, Leandro M., and Marcelo O. Magnasco. "Complex spatiotemporal behavior and coherent excitations in critically-coupled chains of neural circuits." *Chaos: An Interdisciplinary Journal of Nonlinear Science* 28.9 (2018): 093102.
- [15] Solovey, Guillermo, et al. "Self-regulated dynamical criticality in human ECoG." *Frontiers in Integrative Neuroscience* 6 (2012): 44.
- [16] Alonso, Leandro M., et al. "Dynamical criticality during induction of anesthesia in human ECoG recordings." *Frontiers in neural circuits* 8 (2014): 20.
- [17] Solovey, Guillermo, et al. "Loss of consciousness is associated with stabilization of cortical activity." *Journal of Neuroscience* 35.30 (2015): 10866-10877.
- [18] Alonso, Leandro M., et al. "Single-trial classification of awareness state during anesthesia by measuring critical dynamics of global brain activity." *Scientific Reports* 9.1 (2019): 4927. (See also corrigendum).
- [19] Kirst, Christoph, Carl D. Modes, and Marcelo O. Magnasco. "Shifting attention to dynamics: Self-reconfiguration of neural networks." *Current Opinion in Systems Biology* 3 (2017): 132-140.
- [20] Magnasco, Marcelo O. "Robustness and Flexibility of Neural Function through Dynamical Criticality." *Entropy* 24.5 (2022): 591.
- [21] Keller, T. A., Muller, L., Sejnowski, T., & Welling, M. (2023). Traveling waves encode the recent past and enhance sequence learning. arXiv preprint arXiv:2309.08045.
- [22] Karuvally, A., Sejnowski, T. J., & Siegelmann, H. T.



- (2024). Hidden Traveling Waves bind Working Memory Variables in Recurrent Neural Networks. arXiv preprint arXiv:2402.10163.
- [23] Strogatz, Steve; *Nonlinear Dynamics and Chaos: With Applications to Physics, Biology, Chemistry, and Engineering, Second Edition (Studies in Nonlinearity)* (2014)
- [24] Magnasco, Marcelo O. "Convolutional unitary or orthogonal recurrent neural networks." arXiv preprint arXiv:2302.07396 (2023).
- [25] Le, Quoc V., Navdeep, Jaitly, and Hinton, Geoffrey E. A simple way to initialize recurrent networks of rectified linear units. arXiv preprint arXiv:1504.00941, 2015.
- [26] Arjovsky, Martin, Amar Shah, and Yoshua Bengio (2016) "Unitary evolution recurrent neural networks." *International Conference on Machine Learning*. PMLR, 2016.
- [27] Vorontsov, Eugene, et al. "On orthogonality and learning recurrent networks with long term dependencies." *International Conference on Machine Learning*. PMLR, 2017.
- [28] Chang, Bo, et al. "AntisymmetricRNN: A dynamical system view on recurrent neural networks." arXiv preprint arXiv:1902.09689 (2019).
- [29] Saxe, Andrew M., McLelland, James L., and Ganguli, Surya. Exact solutions to the nonlinear dynamics of learning in deep linear neural networks. *International Conference in Learning Representations*, 2014.
- [30] Choromanski, K., Downey, C., & Boots, B. (2018, February). Initialization matters: Orthogonal predictive state recurrent neural networks. In *International Conference on Learning Representations*.
- [31] Hu, W., Xiao, L., & Pennington, J. (2020). Provable benefit of orthogonal initialization in optimizing deep linear networks. arXiv preprint arXiv:2001.05992.
- [32] Kaneko, Kunihiko. "Overview of coupled map lattices." *Chaos: An Interdisciplinary Journal of Nonlinear Science* 2.3 (1992): 279-282.
- [33] Kaneko, Kunihiko. "Theory and applications of coupled map lattices." *Nonlinear science: theory and applications* (1993).
- [34] Nauhaus, I., Busse, L., Carandini, M., & Ringach, D. L. (2009). Stimulus contrast modulates functional connectivity in visual cortex. *Nature neuroscience*, 12(1), 70-76.
- [35] Albrecht DG, Geisler WS, Frazor RA, Crane AM. Visual cortex neurons of monkeys and cats: temporal dynamics of the contrast response function. *Journal of Neurophysiology*. 2002 Aug 1;88(2):888–913. pmid:12163540
- [36] Gawne TJ, Kjaer TW, Richmond BJ. Latency: another potential code for feature binding in striate cortex. *Journal of neurophysiology*. 1996 Aug 1;76(2):1356–60. pmid:8871243
- [37] Zeraati, R., Shi, YL., Steinmetz, N.A. et al. Intrinsic timescales in the visual cortex change with selective attention and reflect spatial connectivity. *Nat Commun* 14, 1858 (2023). <https://doi.org/10.1038/s41467-023-37613-7>